

Stability of Orbits around a Spinning Body in a Pseudo-Newtonian Hill Problem

A. F. Steklain [★] P. S. Letelier ^{★★}

Departamento de Matemática Aplicada, Instituto de Matemática, Estatística e Computação Científica, Universidade Estadual de Campinas, 13083-970, Campinas, São Paulo, Brazil

Abstract

A pseudo-Newtonian Hill problem based on a potential proposed by Artemova et al. [Astroph. J. 461 (1996) 565] is presented. This potential reproduces some of the general relativistic effects due to the spin angular momentum of the bodies, like the dragging of inertial frames. Poincaré maps, Lyapunov exponents and fractal escape techniques are employed to study the stability of bounded and unbounded orbits for different spins of the central body.

Key words: Hill Problem, Chaos, Fractals, Pseudo-Newtonian gravity, Dragging of Inertial Frames

PACS: 04.01A, 05.45

1 Introduction

The Hill Problem was first formulated by Hill [1], in order to study the Moon-Earth-Sun system. This is a special case of the circular, planar restricted three-body problem, as described by Murray and Dermott [2] and Arnold [3], where the movement of the Moon around the Earth was just perturbed by a distant Sun. The Hill Problem is still applied in solar system models where bodies in nearly circular orbits are perturbed by other far away massive bodies, and is very useful in the study of the stellar dynamics. In many systems the Hill problem can be taken as a first approximation and can easily accommodate necessary modifications (see for instance Heggie [4]). The interaction of a Keplerian binary system with a normally incident circularly polarized gravitational wave can be represented by a Hill system,

[★] steklain@ime.unicamp.br

^{★★} letelier@ime.unicamp.br

as shown by Chicone et al. [5]. The Hill problem was proved to be non-integrable by Meletlidou et al. [6], and is chaotic, as shown by Simó and Stuchi [7].

The Hill Problem was first formulated in the context of the Newtonian dynamics. In this dynamics particles or spheres with or without spin have the same gravitational potential. However, on the General Relativity rotation modifies the metric and create effects like the dragging of inertial frames, or Lense-Thirring effect [8]. In General Relativity the exterior field of the simplest meaningful rotating body is described by the Kerr metric [9]. The Schwarzschild metric being the special case of the Kerr metric for spinless bodies.

On a previous work [10], the Hill Problem is study in the framework of a pseudo-Newtonian potential that mimics some properties of the Schwarzschild metric, the Paczyński-Wiita potential [11]

$$\Phi_{PW} = -\frac{GM}{r - r_g}, \quad (1)$$

where G is the gravitational constant, M is the mass of the central body and $r_g = GM/c^2$ is the Schwarzschild or gravitational radius (c is the speed of light). The aim of this work is to study the Hill problem taking into account the spin angular momentum of the central body, with a potential that mimics the dynamics of the Kerr metric. There are several potentials, originally used to study accretion disks around black holes, that fulfill this requirement. Some of this potentials are the Smerak-Karas potential [12] and the Mukhopadhyay potential [13]. However, the potential proposed by Artemova, Björnsson and Novikov (ABN potential) [14] was chosen due to (i) its agreement with the last stable and marginally bound orbits, obtained from the Kerr metric itself; (ii) its simple form, a natural extension of the Paczyński-Wiita potential.

This work can be considered as a “zeroth order” approach to a general relativistic Hill problem with a spinning central body. Due to the complexity of the Einstein equations and its rigorous approximations, like the post-Newtonian expansions, it is worth to begin with this simplified approach to have an idea of the size of the quantities involved. These results can serve as a starting point for a more complete treatment of the problem.

We shall compare the stability of orbits of the third body in the pseudo-Newtonian general relativistic simulation for different spins of the central body with parameters that are typical for a system formed by a supercluster, a galaxy and a star. In this system the influence of the spinning on the dynamics can be easily seen.

2 The ABN Potential

Artemova, Björnsson and Novikov [14] proposed two potentials to use in modeling accretion disks around a rotating black hole. They demanded that their potentials should have three properties: (i) the free-fall acceleration should have the form analogous to the Paczyński-Wiita potential (equation (1)); (ii) the free-fall acceleration must tend to infinity when tends to the event horizon of the black hole; and (iii) the position of the extremum of the boundary condition function must coincide with the position of the last stable circular orbit in the exact relativistic problem. The boundary condition function reads

$$f(r) = 1 - \frac{l_{in}}{l(r)}, \quad (2)$$

where $l(r) = r^2\Omega(r)$ is the Keplerian specific angular momentum at radius r ($\Omega(r)$ is the angular velocity being $\Omega(r) = (GM/r^2)^{1/2}$ for the Newtonian gravitational potential). The constant l_{in} is given by $l_{in} = l(r_{in})$, where r_{in} is the radius of the last stable orbit [14]. The first of the two the free-fall accelerations obtained is of the form

$$F_{ABN} = -\frac{GM}{r^{2-\beta}(r-r_1)^\beta}, \quad (3)$$

or, in the potential form,

$$\Phi_{ABN} = -\frac{GM}{(\beta-1)r_1} \left[\left(\frac{r}{r-r_1} \right)^{\beta-1} - 1 \right], \quad (4)$$

where r_1 is the position of the event horizon. This position is determined from the angular momentum a by the exact expression from general relativity,

$$r_1 = [1 + (1 - a^2)^{1/2}]r_g. \quad (5)$$

The value of β is given from the following equation:

$$\beta = \frac{r_{in}}{r_1} - 1 \quad (6)$$

Where r_{in} is again the last stable orbit. The exact position of this orbit is obtained from the general relativity (see Novikov and Frolov [15], equation 4.5.12),

$$r_{in} = [3 + Z_2 \mp [(3 - Z_1)(3 + Z_1 + 2Z_2)]^{1/2}]r_g, \quad (7)$$

Table 1

Values of r_{mb}/r_g for the ABN potential and Kerr geometry for various values of a

a	0	0.1	0.3	0.5	0.7	0.998
Φ_{ABN}	4	3.797	3.370	2.904	2.376	1.069
Kerr	4	3.797	3.373	2.914	2.395	1.091
a	0	-0.1	-0.3	-0.5	-0.7	-0.998
Φ_{ABN}	4	4.198	4.578	4.942	5.288	5.746
Kerr	4	4.198	4.580	4.949	5.308	5.825

$$Z_1 = 1 + (1 - a^2)^{1/3}[(1 + a)^{1/3} + (1 - a)^{1/3}], \quad (8)$$

$$Z_2 = (3a^2 + Z_1^2)^{1/2} \quad (9)$$

where the upper and the lower signs of the equation (7) are for co-rotation and counter-rotation respectively¹. Note that the parameters r_{in} and β depend only on the angular momentum a .

The radius of the last stable orbit, r_s matches exactly with the last stable orbit in Kerr geometry, as demanded on the construction of this potential. In Table 1 the values of the marginally bound orbit, r_{mb} are listed for the potential above and the Kerr geometry for various values of a . Note that they are in a good agreement with each other. Mukhopadhyay [13] has pointed that using the ABN potential for negative values the error in r_b may be upto 500%. However, if the correct equation for counter-rotation is used (equation (7) with the lower signal), the error in r_b is less than 2%.

For the second potential a different expression for the free-fall acceleration F_{ABN} is obtained. We shall use (4) because it is singular in the event horizon $r = r_1$, like the Paczyński-Wiita potential. The second potential proposed by ABN does not have the above mentioned property.

3 Modified Hill Problem

The Hill problem is a special case of the circular, planar restricted three-body problem, as mentioned before. In this problem there is a system of two massive bodies with masses m_1 and m_2 , in circular orbits around their center of mass and a third massless body moving under influence of this system without perturbing it. In the Hill problem the body with mass m_1 is such that $m_1 \gg m_2$ and is far away of the system, so it constitutes just a perturbation for the two-body system formed by the

¹ In Ref. [14] equation (7) appears only with the minus sign, but the correct form is the above, as in Novikov and Frolov [15].

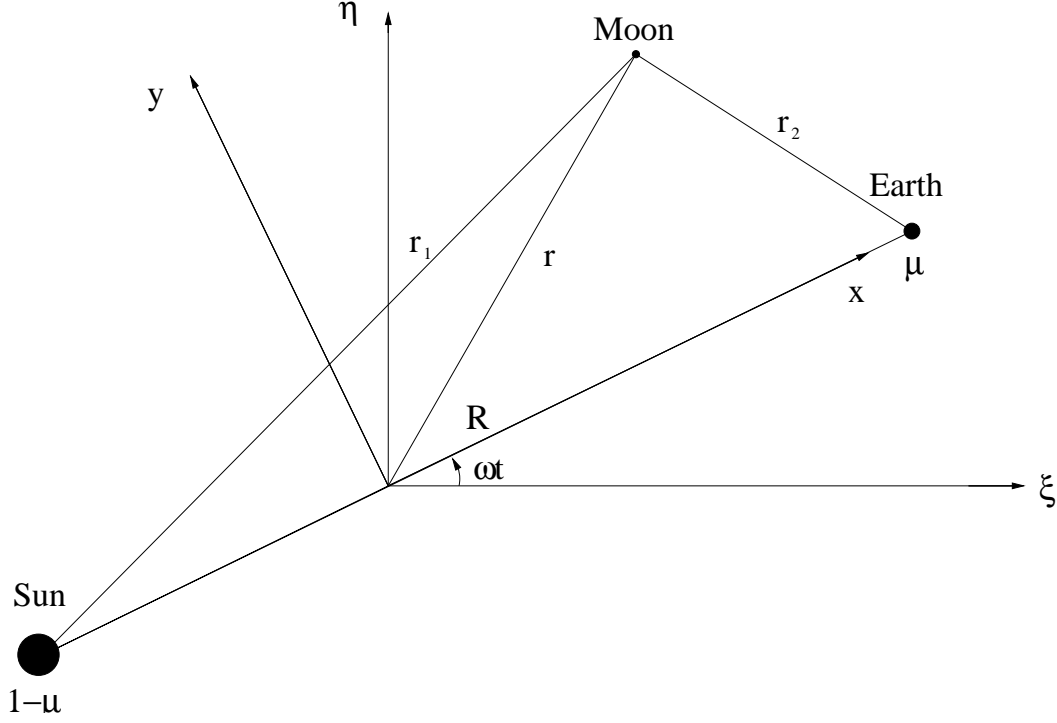


Fig. 1. The planar, circular restricted three-body problem, on a inertial coordinate system (ξ, η) and on a rotating coordinate system (x, y) . Note that on the rotating coordinate system the positions of the two massive bodies are fixed.

body with mass m_2 and the massless body. We can choose units of mass such that $G(m_1 + m_2) = 1$. In this way we can take the units of mass of the two massive bodies respectively as $1 - \mu$ and μ , where $\mu = Gm_2$. We take units of distance such that the distance between the two massive bodies is $R = 1$ and units of time such that the angular velocity of the rotating frame in which the two massive bodies are fixed is $\omega = 1$ (see Fig. 1).

After placing the origin of the coordinate system in the body of mass μ and considering the motion only in a disk of radius $\mu^{1/3}$, we obtain the Newtonian Hill equations [7],

$$\ddot{x} = 2\dot{y} + 3x - \frac{x}{r^3}, \quad (10)$$

$$\ddot{y} = -2\dot{x} - \frac{y}{r^3}, \quad (11)$$

where $r = \sqrt{x^2 + y^2}$. Replacing the Newtonian potential by the ABN potential we obtain the modified Hill equations,

$$\ddot{x} = 2\dot{y} + 3x - \frac{x}{r^{3-\beta}(r - r_1^*)^\beta}, \quad (12)$$

$$\ddot{y} = -2\dot{x} - \frac{y}{r^{3-\beta}(r-r_1^*)^\beta}. \quad (13)$$

These equations can also be written as

$$\ddot{x} - 2\dot{y} = -\frac{\partial U_{ABN}}{\partial x}, \quad (14)$$

$$\ddot{y} + 2\dot{x} = -\frac{\partial U_{ABN}}{\partial y}, \quad (15)$$

where U_{ABN} is the modified Hill potential

$$U_{ABN} = -\frac{3}{2}x^2 - \frac{1}{(\beta-1)r_1^*} \left[\left(\frac{r}{r-r_1^*} \right)^{\beta-1} - 1 \right] = -\frac{3}{2}x^2 + \Phi_{ABN}, \quad (16)$$

and $r_1^* = \mu^{-1/3}r_1$, in units such that the separation between the two massive bodies is $R = 1$, like in the Newtonian case.

The modified Jacobi constant, in this case, is given by

$$C_{JABN} = \frac{1}{2}(\dot{x}^2 + \dot{y}^2) - \frac{3}{2}x^2 - \frac{1}{(\beta-1)r_1^*} \left[\left(\frac{r}{r-r_1^*} \right)^{\beta-1} - 1 \right]. \quad (17)$$

4 Stability of orbits

We shall use for the parameter r_1^* the value $r_1^* = 5.10^{-6}$, that is a typical value for a system formed by a supercluster, a galaxy and a star. We compare the modified Newtonian systems with the angular momentum a varying from -0.5 to 0.5 . The values of β vary, respectively, from 3.05 to 1.27 .

4.1 Fixed points analysis

The Newtonian Hill problem has two well-known fixed points, the Lagrangian points L_1 and L_2 . These points are of saddle-center type, and are located at the positions $(\pm\sqrt[3]{1/3}, 0)$. For the ABN potential it can be guessed that new fixed points, in particular saddle points, arise due to the $r - r_1^*$ dependence of the denominator. However, if the parameter r_1^* is small, the nature of the fixed points remains unchanged. The equation for the x component of the fixed points (obtained by setting $\dot{x}, \dot{y}, \ddot{x}, \ddot{y}$ equal to zero in equations (12) and (13) and replacing $y = 0$) is,

$$|x|^{3-\beta} (|x| - r_1^*)^\beta = \frac{1}{3}. \quad (18)$$

If r_1^* is small compared to x (in this work r_1^* is of order 10^{-6} while x scales as unity) the equation (18) reads, approximately,

$$|x|^3 \left(1 - \beta \frac{r_1^*}{|x|} \right) \approx \frac{1}{3}. \quad (19)$$

For the values of C_J so that the system is bounded, the value of the x component of the fixed points is also bounded. There are one real and two complex conjugate solutions for this approximate equation. For higher values of r_1^* the exact equation (18) can have more than one solution, they may possibly lead to interesting results, but these systems may lack of physical significance.

The Jacobian of the system calculated at the fixed points reads

$$J_F(x_f, y_f) = \begin{pmatrix} 0 & 0 & 1 & 0 \\ 0 & 0 & 0 & 1 \\ 9 + 3\beta \frac{r_1^*}{|x_f| - r_1^*} & 0 & 0 & 2 \\ 0 & -3 & -2 & 0 \end{pmatrix}. \quad (20)$$

The associated characteristic polynomial is

$$(\lambda^2 + 3) \left(\lambda^2 - 9 - 3\beta \frac{r_1^*}{|x_f| - r_1^*} \right) = 0. \quad (21)$$

The eigenvalues are

$$\lambda = \pm i \sqrt{3} \quad (22)$$

$$\lambda = \pm \sqrt{9 + 3\beta \frac{r_1^*}{|x_f| - r_1^*}}. \quad (23)$$

For r_1^* small enough [$r_1^* < 3|x_f|/(3+\beta)$] there are two eigenvalues purely imaginary and two real, so the fixed points are of type *saddle-center*, just as in the Newtonian Hill problem.

4.2 Poincaré sections

The orbits in the Newtonian as well in the modified Newtonian Hill problem are the solutions of a four-dimensional dynamical system with variables (x, y, \dot{x}, \dot{y}) . Since we have an integral of motion, C_{JABN} , the motion is reduced to a three-dimensional

system, we can take (x, \dot{x}, y) as independent variables. We shall study surface of section (Poincaré sections) evaluating the orbits for different values of the Jacobi constant and registering the crossings of the hypersurface $y = 0$ with $\dot{y} > 0$.

The results for $C_J = -2.17$ (typical value for a bounded system) are shown on the Fig. 2. In Fig. 3 there is a magnification of the right portion for the values $a = 0.5$ and $a = -0.5$. We see that, as the angular momentum a increases in modulus (from (a) to (c) and from (d) to (f) in Fig. 2) some Kolmogorov-Arnold-Moser (KAM) tori are deformed and others destroyed, indicating the transition of the system from regular to chaotic behaviour. This transition is more evident for the sequence of negative values of a , i.e., the sequence from (d) to (f), so the destruction of KAM tori is faster for counter-rotation. It means that, for the counter-rotation case, a larger region of the phase space is chaotic when compared with the associated co-rotation system (same angular velocity a in modulus). It does not mean necessarily that the counter-rotating systems are more unstable than the co-rotating ones, since the orbits are still bounded by KAM tori that are not destroyed by the perturbation. Besides, the dependence on initial conditions, the main characteristic of chaotic systems, still must be analyzed by appropriate tools, like Lyapunov exponents. This analysis can decide if a system is more chaotic than other [16].

4.3 Lyapunov exponents

To analyze quantitatively the orbits stability we study the Lyapunov exponents for the systems above described. The Lyapunov characteristic number (λ) is defined as the double limit,

$$\lambda = \lim_{\substack{\delta_0 \rightarrow 0 \\ t \rightarrow \infty}} \left[\frac{\log(\delta/\delta_0)}{t} \right], \quad (24)$$

where δ_0 and δ are the deviation of two nearby orbits at times 0 and t respectively (see Alligood et al. [17]). We get the largest λ using the technique suggested by Benettin et al. [18] and the algorithm of Wolf et al. [19].

The Lyapunov exponents are not absolute, but dependent on the choice of the time scale. We recall that we have fixed the time scale by the requirement that $\omega = 1$. This defines a time unit that is natural to each particular system at it is given in terms of the characteristic period. In this work the analysis is made by varying only the angular momentum a , so the direct comparison between the different Lyapunov exponents is valid. Each coefficient was computed until convergence is reached. To achieve this precision the system of equations was integrated for at least one hundred thousand periods, as shown in Fig. 4. The initial conditions used to perform the integration must be chosen in the bounded region of the system. To estimate the

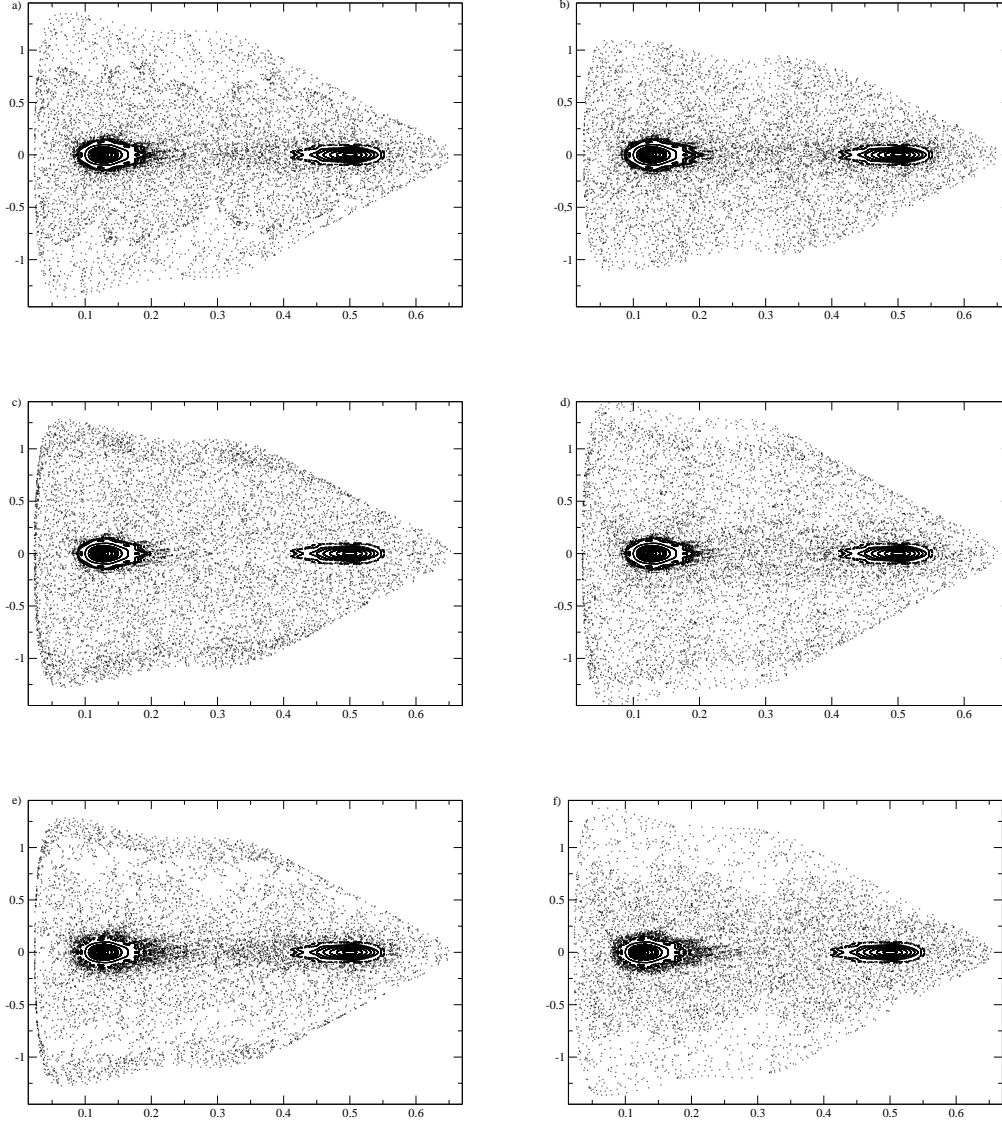


Fig. 2. Poincaré sections for different values of the angular momentum a . Positive values a) $a = 0.1$, b) $a = 0.3$ and c) $a = 0.5$ and negative values d) $a = -0.1$, e) $a = -0.3$ and f) $a = -0.5$. The rate of destruction of KAM tori is greater for the negative values. Note that, for larger values of a , new islands appear in the regular region, indicating transition to chaos.

limit of this region we use the Lagrangian points of the Newtonian Hill system, given numerically by $(\pm 0.69, 0)$. For safety we chose the initial position $(0.3, 0)$. The initial velocity is obtained from the Jacobi constant $C_J = -2.17$, choosing $\dot{x} = 0$. As can be seen in the subsection 4.1 the eigenvalues obtained from the Jacobian of the system remain small, so the system is non-stiff. The calculations are performed with the aid of the Burlisch-Stoer method with step control, that works well for non-stiff systems, and the error due to the integration is proportional to the tolerance imposed (10^{-10}). This relative error is kept small enough, so the

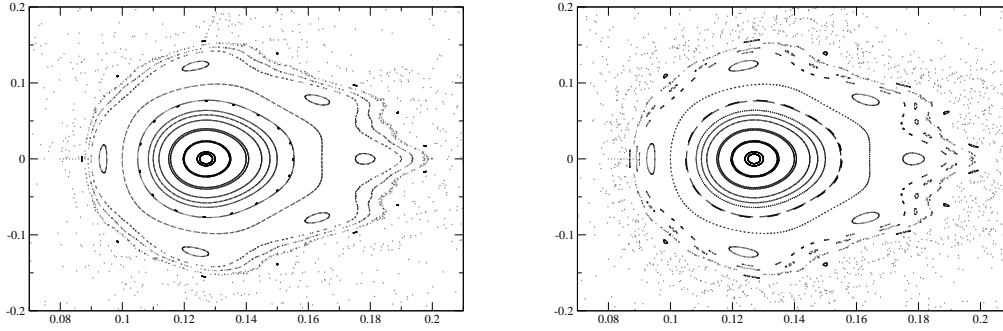


Fig. 3. Magnifications of areas in the Poincaré sections, at left for angular momentum $a = 0.5$ and at right for angular momentum $a = -0.5$. Note that for $a = -0.5$ the tori are more affected by the perturbation.

errors of the coefficients are basically estimate from the fluctuations at the end of each evolution (Fig. 4). The absolute error, according to these fluctuations, is on order of 10^{-8} .

The Lyapunov exponents obtained for this system are shown in Fig. 5. As can be seen from this figure, negatives value of a are associated to a larger Lyapunov exponent when compared with their correspondent positive values. It means that two neighbour orbits separate from each other faster in the counter-rotating system than in the co-rotating system, meaning that the counter-rotating system is more unstable. Nevertheless, this dependence on parameter a is very small for real systems. The reason is the fact that the apparent event horizon is very small when compared with typical distances in the system, and the angular momentum a has only little influence on this horizon as already pointed by Bardeen, Press and Teukolsky [20]. We shall study this dependence in a future work taking another model for the Hill problem closer to the exact general relativistic system.

d) Fractal escape and fractal dimension

The Poincaré sections and Lyapunov exponents were obtained for values of the Jacobi constant such that the systems are bounded. For values larger than $C_{J_{\text{bounded}}} = -2.16$ the systems are unbounded and the third body can escape by two different routes [10]. For open systems that have more than one route to escape we can apply the fractal escape technique used by Moura and Letelier [21] in the study of the classical Hénon-Heiles problem. In this method the basins of the escape routes are obtained for a set of initial conditions. For chaotic systems, we have the existence of fractal basin boundaries (FBB) indicating a great instability of the orbits. In our case we chose a subset of the accessible phase space at a fixed Jacobi constant, defined by a segment $|x| \leq a$, $y = b$ and $0 \leq \theta \leq 2\pi$, where a and b are constants to be chosen appropriately and θ is the angle that defines the direction of the velocity with

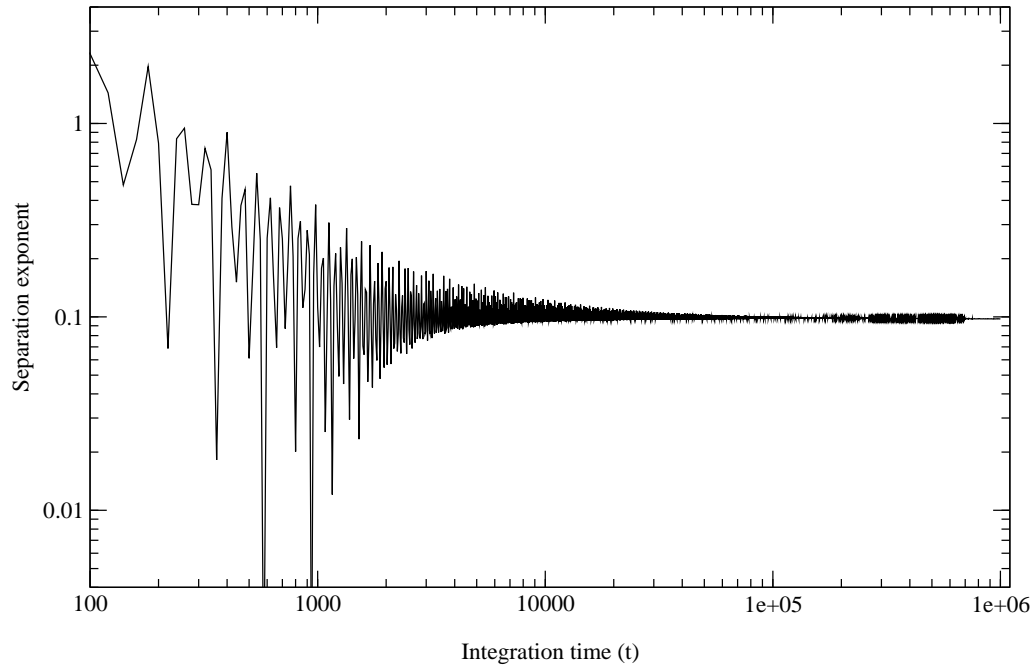


Fig. 4. Time evolution of the separation exponent. It converges to the corresponding Lyapunov characteristic number (λ) for large t .

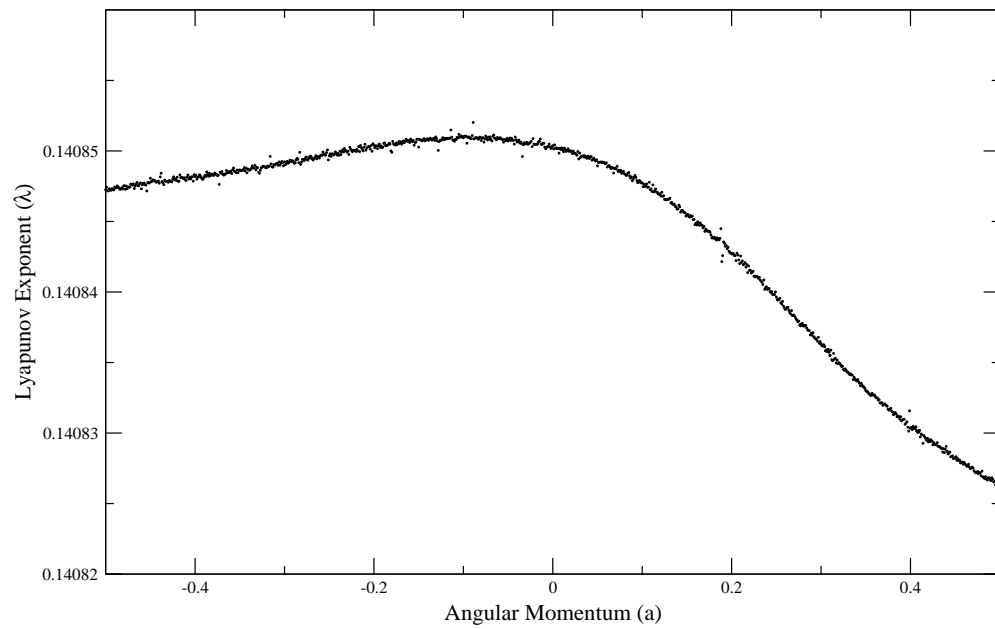


Fig. 5. Lyapunov exponents for different values of a .

respect the x -axis. Then the trajectories are integrated numerically, we have three different cases: (i) the body escapes to $x \rightarrow +\infty$, (ii) it escapes to $x \rightarrow -\infty$, and (iii) the particle does not scape during the integration time. We take the integration time long enough to assure that our results be consistent.

To show the difference between systems with different values of the parameter a , we calculate the dimension of the basin boundaries obtained for the different systems. The dimension used is the box-counting dimension that can be easily obtained, see for instance, Ott [22] and Grebogi et al. [23]. If we displace a determined point of a basin to another on a distance ϵ , the probability that this new initial condition does not belong to the same basin of the old one is, for small ϵ , $P(\epsilon) \propto \epsilon^{D-d}$, where D is the dimension of the set (2 in our case) and d is the box counting dimension, also called exterior or fractal dimension when not integer. In order to calculate this fractal dimension, for several values of ϵ , we displace the x coordinate of all the points from one of the basins ($x \rightarrow +\infty$), and count the number of points that does not belong to the same basin. Then we compute the the fraction of numbers that does not belong to the same basin, $P(\epsilon)$. We plot $\ln P(\epsilon)$ in function of $\ln \epsilon$. The inclination of the straight line gives us $D - d$.

The values for the fractal dimension obtained are shown in the Fig. 6, with error of order $3 \cdot 10^{-3}$. This uncertainty is mainly due to the error in the computation of the line slope. It can be seen that the fractal dimension for negative values of a are larger than the correspondent positive values. The fractal dimension for unbounded systems have a close relationship with the chaoticity of the systems [10],[21], larger fractal dimensions are related to systems that are more unstable. In this sense we can conclude that counter-rotating systems are more unstable than their correspondent co-rotating cases. The validity of this result is limited, as it is applicable only to unbounded systems and the error in calculations are of the order of the variation of data. For bounded systems the analysis of the Lyapunov exponents in the previous section confirms the validity of this result. The values of d are computed only for a few values of a . Is possible that this small density of points can hide a more complex behaviour for this system. Unfortunately to achieve the same density of points used for the Lyapunov exponents is still prohibitive due to the time taken to perform the calculations. We shall improve this method in our future works.

5 Conclusions

In this work we show that we can simulate the dragging of inertial frames by a pseudo-Newtonian potential. We also show, by Poincaré maps, Lyapunov exponents and fractal escape techniques, that there is a dependence of the stability of the orbits on the spin angular momentum of the central body. The bounded and unbounded systems where the movement of particle around the central body is opposite to its spin (counter-rotating) are more unstable than systems where the

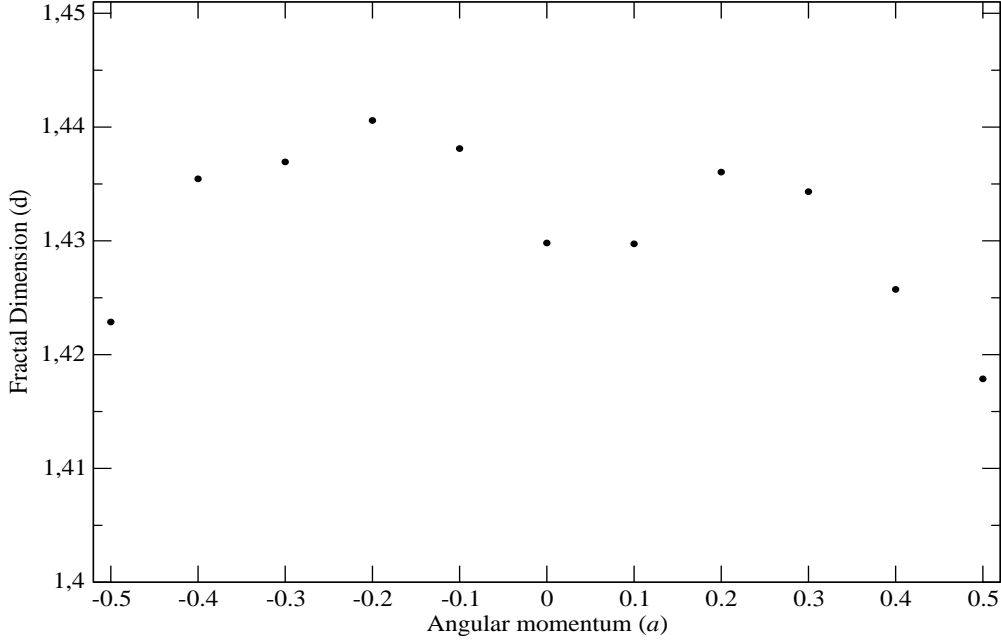


Fig. 6. Fractal dimensions for different values of a .

two rotations are in the same direction (co-rotating). This preliminary result is in accord with previous studies of the stability of orbits of particles moving around spinning centers of attraction [24],[25]. This effect is small when compared with the influence of the position of the event horizon [10]. Otherwise, it can have a larger influence on the Lyapunov exponents. In a future work this feature will be studied in detail to compare the chaoticity of co-rotating and counter-rotating orbits in a full relativistic system, as geodesics in a Kerr black hole with halos [24] or multipolar deformations [25].

6 Acknowledgements

We want to thank CNPq and FAPESP for partial financial support.

References

- [1] G.W. Hill, Am. J. Math. 1 (1878) 129.
- [2] C.D. Murray, S.F. Dermott, Solar System Dynamics, Cambridge Univ. Press, Cambridge, 1999.

- [3] V.I. Arnold, *Mathematical Aspects of Classical and Celestial Mechanics*, Springer-Verlag, Berlin, 1997, p. 88.
- [4] D. Heggie, in: B.A. Steves, A.J. Maciejewski (Eds.), *The Restless Universe*, Scottish Universities Summer School in Physics and Institute of Physics Publishing, Bristol, 2001, p. 109.
- [5] C. Chicone, B. Mashhoon and D.G. Retzloff, *Ann. Inst. H. Poincaré, Phys. Théor.* 64 (1996) 87.
- [6] E. Meletlidou, S. Ichtiaroglou, F.J. Winterberg, *Celest. Mech. Dynam. Astron.* 80 (2001) 145.
- [7] C. Simó, T.J. Stuchi, *Physica D* 140 (2000) 1.
- [8] J. Lense, H. Thirring, *Phys. Z.* 19 (1918) 156.
- [9] R. P. Kerr, *Physic. Rev. Lett.* 11 (1963) 237.
- [10] A.F. Steklain, P.S. Letelier, *Phys. Lett. A* 352 (2006) 398.
- [11] B. Paczyński, P. Wiita, *Astron. Astrophys.* 88 (1980) 23.
- [12] O. Semerák, V. Karas, *Astron. Astrophys.* 343 (1999) 325.
- [13] B. Mukhopadhyay, *Astroph. J.* 581 (2002) 427.
- [14] I.V. Artemova, G. Björnsson, I.D. Novikov, *Astroph. J.* 461 (1996) 565.
- [15] I.D. Novikov, V.P. Frolov, *Physics of Black Holes*, Kluwer, Dordrecht, 1989.
- [16] J.P. Eckmann, D. Ruelle, *Rev. Mod. Phys.* 57 (1985) 617.
- [17] K. Alligood, T. Sauer, J. Yorke, *Chaos - An Introduction to Dynamical Systems*, Springer-Verlag, Berlin, 1996, p. 203.
- [18] G. Benettin, L. Galgani, A. Giorgilli, J.W. Strelcyn, *Meccanica* 15 (1980) 9.
- [19] A. Wolf, J.B. Swift, H.L. Swinney, J.A. Vastano, *Physica D* 16 (1985) 285.
- [20] J.M. Bardeen, W.H. Press, S.A. Teukolsky, *Astroph. J.* 178 (1972) 347.
- [21] A.P.S. Moura, P.S. Letelier, *Phys. Lett. A* 256 (1999) 362.
- [22] E. Ott, *Chaos in Dynamical Systems*, Cambridge University Press, Cambridge, 1993.
- [23] C. Grebogi, H.E. Nusse, E. Ott, J.A. Yorke, in: J.C. Alexander (Ed.), *Dynamical Systems*, Springer-Verlag, Berlin, 1988, p. 220.
- [24] P.S. Letelier, W.M. Vieira, *Phys. Rev. D* 56 (1997) 8095.
- [25] E. Guéron, P.S. Letelier, *Phys. Rev. E* 66 (2002) 046611.